Accepted Manuscript

Title: Mathematical modeling of simultaneous carbon-nitrogen-sulfur removal from industrial wastewater

Author: Xi-Jun Xu Chuan Chen Ai-Jie Wang Bing-Jie Ni Wan-Qian Guo Ye Yuan Cong Huang Xu Zhou Dong-Hai Wu Duu-Jong Lee Nan-Qi Ren

PII: S0304-3894(16)30798-1
DOI: http://dx.doi.org/doi:10.1016/j.jhazmat.2016.08.074
Reference: HAZMAT 18001

To appear in: *Journal of Hazardous Materials*

Received date: 23-12-2015
Revised date: 8-7-2016
Accepted date: 30-8-2016

Please cite this article as: Xi-Jun Xu, Chuan Chen, Ai-Jie Wang, Bing-Jie Ni, Wan-Qian Guo, Ye Yuan, Cong Huang, Xu Zhou, Dong-Hai Wu, Duu-Jong Lee, Nan-Qi Ren, Mathematical modeling of simultaneous carbon-nitrogen-sulfur removal from industrial wastewater, Journal of Hazardous Materials http://dx.doi.org/10.1016/j.jhazmat.2016.08.074

Mathematical Modeling of Simultaneous Carbon-Nitrogen-Sulfur Removal from Industrial Wastewater

Xi-Jun Xu[1], Chuan Chen[1,*], Ai-Jie Wang[1], Bing-Jie Ni[4], Wan-Qian Guo[1],Ye Yuan[1], Cong Huang[1], Xu Zhou[1], Dong-Hai Wu[1], Duu-Jong Lee[1,2,3], Nan-Qi Ren[1,*]

[1]State Key Laboratory of Urban Water Resource and Environment, School of Municipal and Environmental Engineering, Harbin Institute of Technology, P.O. Box 2650, 73 Huanghe Road, Nangang District, Harbin, Heilongjiang Province 150090, China
[2]Department of Chemical Engineering, National Taiwan University, Taipei 106, Taiwan
[3]Department of Chemical Engineering, National Taiwan University of Science and Technology, Taipei 106, Taiwan
[4]Advanced Water Management Centre (AWMC), The University of Queensland, St Lucia, Brisbane, QLD 4072, Australia

[*]corresponding author: echo110244@126.com (Chuan Chen); rnq@hit.edu.cn (Nan-Qi Ren)

Highlights:

1. Simultaneous C-N-S removal from industrial wastewater was mathematically modeled
2. Interactions between SRB, NRB, SOB, FB and MPA were depicted in the model
3. Kinetic parameters for competitive coefficient between SRB and NRB were best estimated
4. The developed mode was the first simulation tool for complicated C-N-S dynamics
5. The model was versatile and feasible to predict relevant processes (e.g., SR-SO, DSR)

ABSTRACT

A mathematical model of carbon, nitrogen and sulfur removal (C-N-S) from industrial wastewater was constructed considering the interactions of sulfate-reducing bacteria (SRB), sulfide-oxidizing bacteria (SOB), nitrate-reducing bacteria (NRB), facultative bacteria (FB), and methane producing archaea (MPA). For the kinetic network, the bioconversion of C-N by heterotrophic denitrifiers ($NO_3^-\rightarrow NO_2^-\rightarrow N_2$), and that of C-S by SRB ($SO_4^{2-}\rightarrow S^{2-}$) and SOB ($S^{2-}\rightarrow S^0$) was proposed and calibrated based on batch experimental data. The model closely predicted the profiles of nitrate, nitrite, sulfate, sulfide, lactate, acetate, methane and oxygen under both anaerobic and micro-aerobic conditions. The best-fit kinetic parameters had small 95% confidence regions with mean values approximately at the center. The model was further validated using independent data sets generated under different operating conditions. This work was the first successful mathematical modeling of simultaneous C-N-S removal from industrial wastewater and more importantly, the proposed model was proven feasible to simulate other relevant processes, such as sulfate-reducing, sulfide-oxidizing process (SR-SO) and denitrifying sulfide removal (DSR) process. The model developed is expected to enhance our ability to predict the treatment of carbon-nitrogen-sulfur contaminated industrial wastewater.

Keywords: mathematical modeling; carbon; nitrogen; sulfur; industrial wastewater treatment

1. Introduction

Agricultural and industrial activities, the rampant land discharge of untreated wastewaters, mostly occurring in urban and rural areas, and leaching from septic tanks are common sources of nitrate. Nitrate contamination of surface water is a relevant problem due to its negative impact on human health, particularly for methemoglobinemia in infants and also nitrate severs as nutrient for photoautotrophs and spurs eutrophication of water bodies [1]. Sulfate is often found as a co-contaminant with nitrate in a variety of waste streams [2-10], as sulfuric acid and sulfate salts are used in many industrial manufacturing processes. Sulfate reduction produces hydrogen sulfide, a corrosive, odorous, and toxic substance [1].

The biological removal of carbon, nitrogen and sulfur that are simultaneously present in waste streams, incorporates several groups of microorganisms, including sulfate-reducing bacteria (SRB), sulfide-oxidizing bacteria (SOB), nitrate-reducing sulfide-oxidizing bacteria (NR-SOB), and heterotrophic nitrate reducing bacteria (NRB) [11-14]. In an anaerobic/anoxic habitat, facultative bacteria (FB) and methane producing archaea (MPA) can co-exist with the other strains for carbon degradation. **Fig. 1** shows the interactions of SRB, SOB, NR-SOB, NRB, FB and MPA in a C-N-S medium and detailed information is presented in the model development section. Considering only the two sequential reactions with SRB (sulfate reduction) and SOB (sulfide oxidation) yields the so-called SR-SO process [15]. Under micro-aerobic conditions (DO<0.5 mg/L), these two steps can be achieved in a single reactor [13], which can be described as the SR-SO process and the O_2OH^- step. The denitrifying

sulfide removal (DSR) process proposed by Chen et al. [12] is equivalent to the two steps R4 and R3 in **Fig. 1**, with sulfide first being oxidized to elemental sulfur by NR-SOB, coupled with the reduction of nitrate to nitrite (R4), followed by the formed nitrite being reduced to N_2 by heterotrophic NRB at the expense of organic carbon oxidation (R3) [16]. Furthermore, Xu et al. [17] proposed a simultaneous desulfurization and denitrification process (SDD), that integrated SR-SO and DSR into one reactor and achieved the simultaneous removal of sulfate and nitrate with lactate as electron donor, accompanying with a high selection rate for sulfur production (>80%) when micro-aerobic conditions were applied.

Complicated interactions between different groups of microorganisms can lead to fruitful reactor dynamics [11, 13, 25-28]. Mathematical modeling has been proven to be an effective tool to understand complex biological wastewater treatment processes. Although simultaneous biological C-N-S removal has been widely studied [14, 15], few efforts have been devoted to modeling the integrated process, especially the synergistic and competitive relationships among microorganisms [48, 51, 53-54]. The Activated Sludge Models Nos. 1, 2 and 3 (ASMs) [18], published by the International Water Association, are able to describe the removal of organic carbon and nitrogen compounds in the reactor (R2 and R3 in Figure 1). Mathematical models have also been applied to predict sulfate removal during industrial wastewater treatment (R1, R6 and R7 in Figure 1) [19-23], as extensions of Anaerobic Digestion Model No. 1 (ADM1) [24]. Furthermore, Fedorovich et al. [55] thoroughly discussed the extension of ADM1 with process of sulfate reduction. Therefore, the work presented here

attempts to model the integrated C-N-S removal process by incorporating ASMs and extended ADM1 with sulfate reduction, and some extensions including oxygen/nitrate-driven sulfide oxidation processes are also considered.

As discussed above, the scheme in **Fig. 1** is a comprehensive model incorporating SR-SO, DSR, SDD, and the interactions of SRB, NRB, (NR-)SOB, FB and MPA. This work constructed a mathematical model of the reaction network in **Fig. 1**, and validated it using batch experimental data. In particular, the kinetic parameters for the competitive coefficient between SRB and NRB were estimated and reported. This proposed model was the first simulation tool for complicated C-N-S dynamics in industrial wastewater treatment.

2. Materials and Methods

2.1 Batch Experimental Data

The sludge used in the batch experiment was cultivated in two laboratory-scale expanded granular sludge bed reactors (EGSB-1 and EGSB-2). Detailed information on the sludge cultivation is given in the SI. Batch experiments were conducted in 300 mL sealable gastight bioreactors, each seeded with 10% v/v sludge from EGSB 1 or EGSB 2. The reactors were flushed with 20 mL min^{-1} argon for 15-20 mins, and then 200 mL pre-prepared medium was added. The tests were conducted at with the bioreactors well mixed throughout all tests by a shaking bath at a speed of 110 rpm, to suspend the sludge in the liquid. Sampling was performed with syringe injection of argon to maintain the gas pressure prior to sampling.

Culture 1: Carbon-Nitrate-Sulfate removal under anaerobic conditions

Three batch tests were performed with sludge from EGSB-1 to investigate carbon-nitrate-sulfate removal under anaerobic condition. The initial nitrate concentrations varied from 200 to 700 mg L^{-1} (**Table 1**), and the initial sulfate and COD concentrations were at 1000 mg L^{-1} and 2700 mg L^{-1}, respectively.

Culture 2: Carbon-Nitrate-Sulfate removal under limited oxygen conditions

In a micro-aerobic environment, six sets of batch tests were performed with sludge from EGSB-2 with initial nitrate, sulfate and COD concentrations of 500 mg L^{-1}, 1000 mg L^{-1} and 2700 mg L^{-1}, respectively. The initial oxygen addition ranged from 20 to 100 mL to generate oxygen to sulfate-sulfur (SO_4^{2-}-S) molar ratio (R_{OS}) of 0.39, 0.77, 1.16, 1.55, or 1.93 (**Table 1**), based on the calculation proposed by Johnston and Voordouw [31]. Restated, using 40.2 mM as the concentration of gaseous oxygen at 30 ºC and 1 atm, the volume (V) of pure oxygen added (at 30 ºC and 1 atm) was as follows:

V = mmol O_2 wanted in solution/ 40.2 mM

=(R_{OS} × mmol SO_4^{2-}-S in initial medium)/40.2 mM

More detailed information about oxygen calculation is given in the SI. The concentration of H_2S in gas phase was ignored in the calculation of R_{OS}.

2.2 Model Development

The developed model included dual-substrate Monod kinetics that synthesized all relevant processes involved in the production and consumption of SO_4^{2-}, NO_3^-, S^{2-}, S^0, NO_2^-, COD, Ac^-, CH_4 and O_2, as described in **Fig. 1**. The model

described the relationships among six biomass groups: SRB (X_{SRB}), heterotrophic NRB (X_{NRB}), SOB (X_{SOB}), MPA (X_{MPA}), FB (X_{FB}), and residual inert biomass (X_I); and nine soluble compounds: SO_4^{2-} (S_{SO4}), NO_3^- (S_{NO3}), S^{2-} (S_{S2}), S^0 (S_{S0}), COD (S_{COD}), Ac^- (S_{AC}), CH_4 (S_{CH4}), O_2 (S_{O2}), and NO_2^- (S_{NO2}). The units were in mg-N L^{-1} for all nitrogenous species, mg-S L^{-1} for all sulfur species, and mg-COD L^{-1} for all other compounds (mg-O_2 L^{-1} for oxygen). To highlight the cycling of nitrogen and sulfur in the waste stream, we selected lactate as the sole carbon source to simplify the carbon metabolism process during the model development and meanwhile SRB prefers the use of lactate for sulfate reduction over acetate, propionate and butyrate based on the Gibbs free energy of sulfate-reducing reactions [41].

In this study, we considered SRB in the bioreactors to be the incompletely degrading type that degraded organic compounds incompletely to acetate (Process 1), because no sulfate reduction was detected when acetate was used as the electron donor instead of lactate in serum bottle tests (data not shown). This result might be due to lactate (in excess) always being utilized as the electron donor during long-term cultivation in bioreactors. Likewise, we assumed that heterotrophic NRB utilized lactate rather than acetate to drive denitrification (Process 2). To describe the inhibition effect of sulfate reduction by nitrate, we employed a competitive-inhibition coefficient in the acceptor part of the dual-substrate Monod kinetics **(Table 2)**. The observation that dissolved oxygen significantly inhibited the denitrification rate [39] was described by multiplying the corresponding kinetic rate by a substrate inhibition function for O_2,

and this study employed one parameter ($K_{I,O2}^{NRB}$) to represent the O_2 inhibition coefficient for both the denitratation and denitritation processes due to their relatively close values, as reported in Henze et al. [18]

Process 1: Heterotrophic SO_4^{2-} reduction

$$SO_4^{2-} + 2C_3H_5O_3^- + 4OH^- \rightarrow S^{2-} + 2CH_3COO^- + 2CO_3^{2-} + 4H_2O \quad (R1)$$

Process 2: Heterotrophic denitrification

$$6NO_3^- + C_3H_5O_3^- \rightarrow 6NO_2^- + 3CO_2 + OH^- + 2H_2O \quad (R2)$$

$$4NO_2^- + C_3H_5O_3^- \rightarrow 2N_2 + 3CO_2 + 5OH^- \quad (R3)$$

As indicated above, as there was sufficient support for elemental sulfur as the dominant end-product of sulfide oxidation when the electron acceptor was limited [25, 26], SOB mediated sulfide oxidation to sulfate was ignored in our model.

Process 3: S^{2-}-driven autotrophic denitrification

$$S^{2-} + NO_3^- + 2H^+ \rightarrow S^0 + NO_2^- + H_2O \quad (R4)$$

Process 4: Microaerobic S^{2-} oxidation

$$2HS^- + O_2 \rightarrow 2S^0 + 2OH^- \quad (R5)$$

Additionally, hydrogen-utilizing methanogens were easily and rapidly out-competed by SRB due to their higher affinity and lower threshold values, and the analysis of microbial communities in Cultures 1 and 2 also indicated that relative abundance of acetate-utilizing methanogens (e.g., *Methanosaeta*, *Methanosarcina*) exceeded 98% **(Table S1)**. Thus homoacetogens utilized COD as a substrate to produce only acetate but no hydrogen gas (Process 6) and methane production was almost completely via Process 5. The inhibitory effect of nitrate on methanogenesis was initially included in

the model, but impacted little on the result for the scenarios tested which was in accordance with previous findings [42, 43] and was therefore omitted to reduce the complexity of the model. The aerobic COD oxidation process performed by FB was considered based on the biochemical reactions R8 and R9 below.

Process 5: Acetate-utilizing methanogenesis

$CH_3COOH \rightarrow CH_4 + CO_2$ (R6)

Process 6: Homoacetogenic reaction

$C_3H_5O_3^- \rightarrow 1.5CH_3COO^- + 0.5H^+$ (R7)

Process 7: Aerobic lactate/acetate oxidation

$3O_2 + C_3H_6O_3 \rightarrow 3CO_2 + 3H_2O$ (R8)

$2O_2 + C_2H_4O_2 \rightarrow 2CO_2 + 2H_2O$ (R9)

The initial conditions for the dynamic simulation were estimated as recommended by Rieger et al. [52]. In brief, the inoculums for batch tests were withdrawn from steady-state bioreactor, and according to the continuous bioreactor influent, sludge retention time (SRT), microorganism yield efficiency, specific maximum growth rate and decay efficiency, each microorganism concentration at steady state bioreactor (also initial microorganism concentration) can be estimated by Lawrence-McCarty formula. Herein, the initial concentrations of various biomass groups were estimated to be (in mg/L): 5900 (X_{SRB}), 2100 (X_{NRB}), 0.5 (X_{SOB}), 1000 (X_{MPA}), and 100 (X_{FB}), respectively. The kinetics and stoichiometry of the interactions and transformations among model components are listed in **Table 2**. **Table 3** lists the definition, values, and units of the parameters used in the model.

2.3 Parameter Estimation, Uncertainty Analysis and Model Validation

Parameter estimation was performed using Matlab (2006) (Mathworks, Inc., USA). The parameter values were estimated by minimizing the sum of squares of the deviations between the measured data and the model predictions using the objective function [36]. The parameter uncertainty was evaluated according to the method of Batstone et al. [45], with a 95% confidence level for significance testing and parameter uncertainty analysis. The mean square error (MSE) of a fitting parameter, which was used to calculate the 95% confidence interval of a given parameter estimate, was calculated from the mean square fitting error and the sensitivity of the model to the parameter [36]. Detailed information on the method for parameter estimation is given in the SI.

2.4 Sampling and Analytical Methods

Mixed liquid samples were taken at given intervals using a syringe and were filtered through disposable Millipore filter units ($0.22\ \mu m$ pore size) before measurement. Using a Waters High Performance Liquid Chromatography (HPLC), lactate and volatile fatty acid (e.g., acetate and propionate) concentrations were determined with a Bio-RAD Carbohydrate analysis column (Aminex, HPX-87P, 300 ×7.8 mm) with deionized water eluent flowing at 0.6 mL min-1 and a Waters 2489 UV/Visible detector at 220 nm. The concentrations of SO_4^{2-}, NO_3^-, NO_2^-, and $S_2O_3^{2-}$ were determined with a ion chromatography (ICS-3000, Dionex, Bannockbum, IL, USA) [12]. The concentration of aqueous sulfide was determined spectrophotometrically (UV759S, Shanghai, China) with N,

N-dimethyl-p-phenylenediamine [31]. The concentrations of gaseous species in the headspace (CH_4, O_2, N_2) were determined with a gas chromatography (GC-6890, Agilent, Foster City, CA, USA) [12]. The measurement of MLVSS and COD was performed according to the Standard Methods [49]. $ZnCl_2$ was added to the samples to eliminate sulfide-induced interference prior to COD measurement. The detailed procedure for microbial community analysis is given in SI.

3. Results

3.1 Carbon-Nitrate-Sulfate removal in batch tests

Fig. 2 and Fig. 3 show the batch test results. Carbon, nitrate and sulfate were almost completely removed in both Cultures 1 and 2. NO_2^- or $S_2O_3^{2-}$ accumulation was not observed in all tests, suggesting that the bioreactor was not carbon-limited and that the sulfide oxidation observed in Culture 2 was mainly attributable to bio-oxidation process [29]. Furthermore, ammonium production was not detected in this study, although some SRB are capable of reducing nitrate to ammonium [44], and thus nitrate use by SRB was not included in the model. An inhibitory effect of nitrate on sulfate reduction was clearly shown in Culture 1 where an increase in the initial nitrate concentration prolonged the lag phase in sulfate reduction, which was consistent with previous findings [7, 30]. This observation was also consistent with the acetate profiles (**Fig. 2**), in which acetate was accumulated with decreased initial nitrate concentration, and acetate production was assumed to be mainly coupled with sulfate reduction. For Culture 2, a noticeable impact of R_{OS} on sulfide oxidation was observed and this impact was increased with the increment of R_{OS} (**Fig. 3**). R_{OS}

determines the end-products of sulfide oxidation [25, 26]. At R_{OS}=1.93, complete sulfide oxidation was observed. The stoichiometry $2H_2S + O_2 \rightarrow 2S^0 + 2H_2O$ indicated that all sulfide could be converted to sulfur at R_{OS}>0.5. The fact that complete sulfide conversion to sulfur was only observed at R_{OS} of 1.93 or higher suggested that in addition to sulfide oxidation, part of the oxygen consumption was likely used for carbon oxidation [28, 31]. Furthermore, the micro-aerobic conditions resulted in a decreased nitrate reduction rate; however, a slight increase in sulfate reduction rate was also observed (**Fig. 3**).

Methanogenesis is progressively inhibited with the increase of sulfide concentration in the substrate and this inhibition is related to the undissociated H_2S concentration (affected by pH) [24]. In our tests, the pH of the medium was adjusted to 8.0 ± 0.1 by the addition of sodium bicarbonate, and the undissociated H_2S concentration was ignored. Therefore the undissociated H_2S inhibition showed little effect on methanogenesis. Moreover, methane production was observed in all tests regardless of R_{OS} (**Fig. 3**). Although methanogens are extremely oxygen-sensitive, the presence of active methanogens indicated the formation of a local niche without oxygen, and oxygen was speculated to be consumed via chemical reduction with H_2S that might be formed by the nearby SRB or through dissimilatory sulfur reduction process [32]. Methanogens have been found to survive in the presence of dissolved oxygen and to coexist with aerobic or microaerophilic organisms [33].

3.2 Model Calibration and Validation for Culture 1

The four key parameters, $\mu_{An,FB}$, K_S^{SRB}, $K_{I,NO3}^{SRB}$, and $K_{I,SO4}^{NRB}$ in this model were

estimated by fitting simulation results to the experimental data from Culture 1 with an initial nitrate concentration of 500 mg L^{-1} (**Table 3**). The close agreement between the model simulations and the measured sulfate, nitrate, sulfide, acetate, methane and lactate data (**Fig. 2**) confirmed the validity of the proposed model for describing the dynamics of sulfate reduction, nitrate reduction, carbon oxidation, acetate accumulation and methane production. The estimated $\mu_{An,FB}(0.18 \pm 0.03\ h^{-1})$ was of the same order of magnitude and commensurate with a typical maximum FB growth rate value of 0.1-0.2 h^{-1} [34]. The calibrated K_S^{SRB} value of 18.5 ± 2.0 mg COD L^{-1} was much higher than K_S^{NRB} (5.0 mg COD L^{-1}), reflecting a higher carbon affinity for nitrate reduction than sulfate reduction. Competitive-coefficient ($K_{I,NO3}^{SRB}$, $K_{I,SO4}^{NRB}$) parameters were incorporated in this model during nitrate and sulfate reduction. The competition between incompletely degrading type SRB and MPA was not considered in the model due to the excess of lactate as the sole organic carbon in the medium. Model validation was conducted based on model predictions and batch experimental data at initial nitrate concentrations of 200 and 700 mg L^{-1}. The comparison in **Fig. 2** shows that the model predictions fit the measured data at the two different initial nitrate concentrations without systematic deviation. The correlation between the independent data sets and model predictions supported the validity of the developed model for C-N-S removal.

3.3 Model Calibration and Validation for Culture 2

The seven key parameters, $\mu_{An,FB}$, K_S^{SRB}, $K_{I,NO3}^{SRB}$, $K_{I,SO4}^{NRB}$, $K_{I,O2}^{SRB}$, $K_{I,O2}^{NRB}$, and $K_{I,O2}^{MPA}$ that govern the sulfate and nitrate reduction in micro-aerobic conditions were

estimated by fitting the simulation results to the experimental data collected in batch test at R_{OS}=1.16. **Fig. 3** reveals the close correlation between the simulation and experimental results. In the model calibration, the data for elemental sulfur were estimated by mass balance calculation [13]. Additionally, parameter values related to sulfide oxidation and oxygen consumption were available in the literature and were adopted as provided.

Calibrated parameters are listed in **Table 3**. The obtained parameter values of $\mu_{An,FB}$, and K_S^{SRB}were 0.16 ± 0.02 h^{-1} and 15.7 ± 3.5mg COD L^{-1}, respectively, which were comparable to the values obtained for Culture 1. Nevertheless, the values of $K_{I,NO3}^{SRB}$ and $K_{I,SO4}^{NRB}$ obtained here deviated from the values obtained in Culture 1, whose mechanisms are discussed in Sec. 4.2. The oxygen inhibition coefficient for sulfate reduction ($K_{I,O2}^{SRB}$) and methanogenesis ($K_{I,O2}^{MPA}$) seemed notably higher than reported, indicating a high tolerance of SRB and MPA for oxygen herein. This result might be due to the rapid oxygen depletion by SOB and FB, limiting the exposure of SRB and MPA to oxygen and this oxygen shielding effect may explain the viability of constant methane production for the scenarios tested. Likewise, due to rapid oxygen consumption by several groups of microorganisms in the bioreactor, the oxygen inhibition coefficient for nitrate/nitrite reduction ($K_{I,O2}^{NRB}$) was relatively higher than the reported values (0.087 and 0.1 mg L^{-1}) [18]. This inhibition coefficient parameter represented a combined interaction between NRB and other oxygen-uptake microorganisms. The inhomogeneity of the culture, which may be attributed to clumping by the bacteria, has been considered to be responsible for the creation of

anaerobic micro-niches that allow denitrification. Bacteria coexist and interact with each other, forming consortia taht drive key biogeochemical cycles. Model predictions with best-fit parameters are shown in **Fig. 3** for comparison with four data sets at R_{OS} of 0.39, 0.77, 1.55, and 1.93. The model again properly described the C-N-S removal under micro-aerobic condition.

4. Discussion

4.1 Complexity and Identifiability of the Proposed Model

Parameter identifiability was revealed by analyzing the 95% confidence intervals of the individual parameter estimate and the joint confidence regions for different parameter combinations [35]. **Fig. 4** shows the parameter surfaces that bound the 95% confidence regions for all the pairs of parameter combinations from both Cultures 1 and 2. The maximum anaerobic growth rate of FB ($\mu_{An,FB}$) was between 0.13 and 0.23 h^{-1}, with a narrow confidence interval (0.15-0.21 h^{-1}) for Culture 1, and between 0.13 and 0.19 h^{-1} with a narrow confidence interval (0.14-0.18 h^{-1}) for Culture 2. The high-overlap confidence regions in Culture 1 and 2 indicated a good consistency of the calibrated $\mu_{An,FB}$ in different conditions. Conversely, the values of $K_{I,NO3}^{SRB}$ and $K_{I,SO4}^{NRB}$ were in the ranges of 225.8 ± 20.3 mg N L^{-1} (277.5 ± 18.9 mg N L^{-1}, Culture 2) and 327.3 ± 68.7 mg S L^{-1} (267.1 ± 33.3 mg S L^{-1}, Culture 2), with confidence intervals of 195-255 mg N L^{-1} (250-305 mg N L^{-1}, Culture 2) and 240-425 mg S L^{-1} (225-315 mg S L^{-1}, Culture 2), respectively. The weak-overlap confidence regions observed in both cultures suggested a culture-specific characteristic of $K_{I,NO3}^{SRB}$

and $K_{I,SO4}^{NRB}$ and the estimation and application depended heavily on actual operating conditions. Overall, the 95% confidence regions for each of the pairs considered were bound by small ellipsoid with the mean value of the parameter estimates lying at the center, confirming the identifiability of these parameters (**Fig. 4**). Furthermore, none of the 95% confidence ellipsoids extended more than ±20% from the best-fit values (mostly <15%), and the 95% confidence intervals for each parameter did not extend more than ±30% from the best-fit values (mostly < 20%), which indicated good identifiability of these parameters (**Fig. 4**).

4.2 Biomass at Steady States

To better understand the microbial ecology of these relevant bacteria across different R_{OS} conditions, we modeled the biomass distribution at steady state in a continuous reactor, with the same input conditions as in Culture 2 (**Table 1**). At steady state, the mass of solid components decayed from the sludge equaled the net yield production of all solid components in the biomass. Thus the steady-state biomass concentrations (i.e. X_{NRB}, X_{SRB}, X_{SOB}, X_{MPA}, X_{FB}) at R_{OS} ranging from 0.39 to 1.93 were determined through calculations (iterations) in the model (adding an advective term, $Q X_0/V - Q X/V$, to the chemostat mass balance equation, where V is the liquid volume, Q is the flow rate, and X_0 and X represent the initial and steady-state biomass concentrations). More details are available in Ni et al. [35] The estimated total biomass across the six steady states was as follows: $6 > 5 \approx 4 \approx 3 > 2 > 1$. The SRB numbers were as follows: $3 > 2 > 4 > 5 > 6 > 1$, indicating larger SRB populations in the presence of oxygen, which matched the experimental

observations. Anaerobic SRB can survive or even take advantage in the presence of molecular oxygen [37]. However, the estimated NRB numbers, $6 > 5 \approx 4 \approx 3 > 2 > 1$, did not correlate with the experimental findings [38], and the most significant discrepancy lay in the fact that the estimated NRB numbers increased with R_{OS}, while the observed nitrate reduction rate decreased with increasing R_{OS}. One possible explanation for the inconsistency was that the increased NRB numbers could be attributed to oxygen supply. Restated, the shift of excess NRB to oxygen reduction instead of the nitrate reduction pathway decreased the nitrate reduction rate despite the substantial increase in NRB numbers with R_{OS}. This possibility was proposed based on the fact that oxygen appeares to be available as an alternative and energetically preferable electron acceptor for facultative denitrifying bacteria, and has been shown to regulate the synthesis of nitrate reductase enzyme and inhibit denitrification in pure cultures of facultative denitrifying bacteria so that substrate electrons flow to oxygen cytochromes [39]. As expected, the SOB numbers followed exactly the same trends as the experiments and model: $6 > 5 > 4 > 3 > 2 > 1$. Higher R_{OS} led to higher SOB numbers, and the intensive sulfide oxidation level suggested a significant enhancement of SOB growth under limited-oxygen.

4.3 Implication of This Work

The proposed model was also feasible for evaluating other system dynamics, such as sulfate-reduction (SRB), sulfide-oxidation (SOB), sulfate-reduction, the sulfide-oxidation process (SR-SO), the denitrifying sulfide removal process (DSR) and the simultaneous desulfurization and denitrification removal process (SDD). Thus,

we performed further simulation using the proposed pathway (R1-R9) (switching off some pathways whenever needed) and calibrated the parameter values. For example, to model the SR-SO system, we set the initial nitrate concentration to zero and combined processes R1 and R5-R9 for modeling. The parameters for the model simulation are derived directly from **Table 3,** and parametric optimization could be performed as needed. Likewise, when we ran the model simulation for the DSR system, the initial conditions for simulation were the same as indicated above except that the initial sulfate concentration was zero and processes R2-R5 were combined. **Fig. 5** plots the simulation results and experimental data (derived from Xu et al. [28] and Chen et al. [40]) for the SR-SO and DSR processes, respectively and once again, the good agreement between them suggested a feasible use of the proposed model.

The ability to predict C-N-S removal by modeling provides an opportunity to explore the effect of operational parameters on removal dynamics and forms the basis for the design and operational optimization of a biological C-N-S removal process. In our model, methane production from H_2 is not considered. This simplification may be revised in the future, if more information on the consumption of H_2 by hydrogenotrophic methanogens becomes available. The model also ignores the occurrence of some precipitation in the presence of SO_4^{2-} in real wastewater. As a result, the model may not be able to describe all experimental observations. Furthermore, in real wastewater, the organic carbon constituent is much more complex than lactate, and it may be not safe to apply the proposed model to capture C-N-S dynamics in real wastewater. However, these “weak points” can be improved

in future work on model calibration and validation with long-term studies and using different carbon sources representative of a large scale real system. While this model may not yet serve as a precise and quantitative predictor in various full-scale C-N-S removal applications (due to parameter value uncertainty), it can nevertheless serve as a tool to provide theoretical guidance for ongoing refinements and confirm the consensus mechanism of enhanced S^0 production under limited oxygen condition.

5. Conclusions

A mathematical model considering the simultaneous removal of carbon, nitrogen and sulfur from industrial wastewater was developed by combination of ASMs and extended ADM1 accompanied with some extensions including oxygen/nitrate-driven sulfide oxidation processes. The kinetic behaviors of sulfur, nitrogen and carbon compounds with the growth of several functional bacteria including SRB, NRB, (NR-)SOB, FB and MPA were considered, and the model described the dynamic processes for C-N-S removal well. The model output under micro-aerobic conditions suggested a possible microbial structure response mitigating toxic sulfide emission to the environment. While this model may not yet serve as a precise and quantitative predictor in various full-scale applications (due to some simplifications made in the model), it can nevertheless serve as tool to explore the effect of operational conditions on performance and confirm the consensus mechanism of enhanced S^0 production under limited oxygen condition.

Acknowledgements

This research was supported by the National Natural Science Foundation of China (Grant No. 51576057 and 51308147), Fundamental Research Funds for Central Universities (AUGA5710055514), Natural Scientific Research Innovation Foundation in Harbin Institute of Technology (HIT.NSRIF.2015094), National High-tech R&D Program of China (863 Program, Grant No. 2011AA060904), Open Project of State Key Laboratory of Urban Water Resource and Environment, Harbin Institute of Technology (No. HC201526-02), and Shanghai Tongji Gao Tingyao Environmental Science & Development Foundation. Bing-Jie Ni acknowledges the supports of Australian Research Council Discovery Project (DP130103147).

Reference

[1] A.O. Valencia, M.Z. El, H.P. Zhao, L. Feng, B.E. Rittmann, R. Krajmalnik-Brown, Interactions between nitrate-reducing and sulfate-reducing bacteria coexisting in a hydrogen-fed biofilm. Environ. Sci. Technol. 46 (2012) 11289-11298.

[2] M.D. Krom, A.B. David, E.D. Ingall, L.G. Benning, S. Clerici, S. Bottrell, C. Davies, N.J. Potts, R.J.G. Mortimer, J. van Rijn, Bacterially mediated removal of phosphorus and cycling of nitrate and sulfate in the waste stream of a "zero-discharge" recirculating mariculture system. Water Res. 56 (2014) 109-121.

[3] D. Kaown, D.C. Koh, B. Mayer, K.K. Lee, Identification of nitrate and sulfate sources in groundwater using dual stable isotope approaches for an agricultural area with different land use (Chunchaeon, mid-eastern Korea). Agric. Ecosyst. Environ. 132 (2009) 223-231.

[4] Q. Li, B. Huang, X. Chen, Y. Shi, Cost-effective bioregeneration of nitrate-laden ion exchange brine through deliberate bicarbonate in incorporation. Water Res. 75 (2015) 33-42.

[5] A. Keranen, T. Leiviska, O. Hormi, J. Tanskanen, Removal of nitrate by modified pine sawdust: effects of temperature and co-existing anions. J. Environ. Manage. 147 (2014) 46-54.

[6] J.M. Zhou, Z.Y. Song, D.J. Yan, Y.L. Liu, M.H. Yang, H.B. Cao, J.M. Xing, Performance of a haloalkaliphilic bioreactor under different NO_3^-/SO_4^{2-} ratios. Bioresour. Technol. 153 (2014) 216-222.

[7] C. Hubert, G. Voordouw, B. Mayer, Elucidating microbial processes in nitrate- and sulfate-reducing systems using sulfur and oxygen isotope ratios: the example of oil reservoir souring control. Geochim. Cosmochim. Acta 73 (2009) 3864-3879.

[8] S. Gandhi, B.T. Oh, J.L. Schnoor, P.J.J. Alvarez, Degradation of TCE, Cr (VI), sulfate, and nitrate mixtures by granular iron in flow-through columns under different microbial conditions. Water Res. 36 (2002) 1973-1982.

[9] R.M. Awadallah, M.E. Soltan, S.A. Shabeb, S.M.N. Moalla, Bacterial removal of nitrate, nitrite and sulfate in wastewater. Water Res. 32 (1998) 3080-3084.

[10] A. Wiessner, U. Kappelmeyer, P. Kuschk, M. Kastner, Sulfate reduction and the removal of carbon and ammonia in a laboratory-scale constructed wetland. Water Res. 39 (2005) 4643–4650.

[11] L.B. Celis-Garcia, G. Gonzalez-Blanco, M. Meraz, Removal of sulfur inorganic compounds by a biofilm of sulfate reducing and sulfide oxidizing bacteria in a down-flow fluidized bed reactor. J. Chem. Technol. Biotechnol. 83 (2008) 260-268.

[12] C. Chen, N.Q. Ren, A.J. Wang, Z.G. Yu, D.J. Lee, Simultaneous biological removal of sulfur, nitrogen and carbon using EGSB reactor. Appl. Microbial. Biotechnol. 78(6) (2008) 1057-1063.

[13] X.J. Xu, C. Chen, A.J. Wang, N. Fang, Y. Yuan, N.Q. Ren, D.J. Lee, Enhanced elementary sulfur recovery in integrated sulfate-reducing, sulfur-producing reactor under micro-aerobic condition. Bioresour. Technol. 116 (2012) 517-521.

[14] K.Y. Show, D.J. Lee, X.L. Pan, Simultaneous biological removal of nitrogen-sulfur-carbon: Recent advances and challenges. Biotechnol. Adv. 31 (2013) 409–420.

[15] P.N.L. Lens, A. Visser, A.J.H. Janssen, L.W. Hulshoff, G. Lettinga, Biotechnological treatment of sulfate-rich wastewaters. Environ. Sci. Technol. 28 (1998) 41-88.

[16] J. Reyes-Avila, E. Razo-Flores, J. Gomez, Simultaneous biological removal of nitrogen, carbon and sulfur by denitrification. Water Res. 38 (2004) 3313-3321.

[17] X.J. Xu, C. Chen, A.J. Wang, H. Yu, X. Zhou, H.L. Guo, Y. Yuan, D.J. Lee, J.Z. Zhou, N.Q. Ren, Bioreactor performance and functional gene analysis of microbial community in a limited-oxygen fed bioreactor for co-reduction of sulfate and nitrate with high organic input. J. Hazard. Mater. 278 (2014) 250–257.

[18] M. Henze, W. Gujer, T. Matsuo, M.C.M. van Loosdrecht, Activated Sludge Models ASM1, ASM2, ASM2d and ASM3, Scientific and Technical Reports; IWA Publishing: London (2000).

[19] S.V. Kalyuzhnyi, V.V. Fedorovich, Mathematical modeling of competition between sulfate reduction and methanogenesis in anaerobic reactors. Bioresour. Technol. 65 (1998) 227-242.

[20] A.N. Knobel, A.E. Lewis, A mathematical model of a high sulfate wastewater anaerobic treatment system. Water Res. 36 (2002) 257-265.

[21] S. Moosa, M. Nemati, S.T.L. Harrison, A kinetic study an anaerobic reduction of sulfate, Part I: effect of sulfate concentration. Chem. Eng. Sci. 57 (2002) 2773-2780.

[22] O.O. Oyekola, R.P. van Hille, S.T.L. Harrison, Kinetic analysis of biological sulfate reduction using lactate as carbon source and electron donor: effect of sulfate concentration. Chem. Eng. Sci. 65 (2010) 4771-4781.

[23] C.M. Moon, R. Singh, S.R. Chaganti, J.A. Lalman, Modeling sulfate removal by inhibited mesophilic mixed anaerobic communities using a statistical approach. Water Res. 47 (2013) 2341-2351.

[24] D.J. Batstone, J. Keller, I. Angelidaki, S.V. Kalyuzhnyi, S.G. Pavlostathis, A. Rozzi, W.T.M. Sanders, H. Siegrist, V.A. Vavilin, Anaerobic Digestion Model No.1. (ADM1). IWA Publishing, London. IWA Scientific and Technical Report No. 1 (2002).

[25] A.J.H. Janssen, P. Lens, S.C. Ma, G. Lettinga, Performance of a sulfide-oxidizing expanded-bed reactor supplied with dissolved oxygen. Biotechnol. Bioeng. 53 (1997) 32-40.

[26] S. Alcantara, A. Velasco, A. Munoz, J. Cid, S. Revah, E. Razo-Flores, Hydrogen sulfide oxidation by a microbial consortium in a recirculation reactor system: sulfur formation under oxygen limitation and removal of phenols. Environ. Sci. Technol. 38 (2004) 918-923.

[27] E. Sahinkaya, H. Hasar, A.H. Kaksonen, B.E. Rittmann, Performance of a sulfide-oxidizing, sulfur-producing membrane biofilm reactor treating sulfide-containing bioreactor effluent. Environ. Sci. Technol. 45 (2011) 4080-4087.

[28] X.J. Xu, C. Chen, D.J. Lee, A.J. Wang, W.Q. Guo, X. Zhou, H.L. Guo, Y. Yuan, N.Q. Ren, J.S. Chang, Sulfate-reduction, sulfide-oxidation and elemental sulfur bioreduction process: Modeling and experimental validation. Bioresour. Technol. 147 (2013) 202-211.

[29] A.H. Nielsen, T. Hvitved-Jacobsen, J. Vollertsen, Kinetics and stoichiometry of sulfide oxidation by sewer biofilms. Water Res. 39 (2005) 4119-4125.

[30] K.M. Kaster, A. Grigoriyan, G. Jenneman, G. Voordouw, Effect of nitrate and nitrite on sulfide production by two thermophilic, sulfate-reducing enrichments from an oil field in the North Sea. Appl. Microbial. Biotechnol. 75 (2007) 195-203.

[31] S.L. Johnston, G. Voordouw, Sulfate-reducing bacteria lower sulfur-mediated pitting corrosion under conditions of oxygen ingress. Environ. Sci. Technol. 46 (2012) 9183-9190.

[32] K.O. Stetter, G. Gaag, Reduction of molecular sulfur by methanogenic bacteria. Nature, 305 (1983) 309-311.

[33] D.H. Zitomer, J.D. Shrout, Feasibility and benefits of methanogenesis under oxygen-limited conditions. Waste Manage. 18 (1998) 107-116.

[34] D.R. Boone, M.P. Bryant, Propionate-degrading bacterium, Syntrobacter wolinii sp. nov.gen. nov., from methanogenic ecosystems. Appl. Environ. Microbial. 40 (1980) 626-632.

[35] B.J. Ni, M. Ruscalleda, C. Pellicer-Nacher, B.F. Smets, Modeling nitrous oxide production during biological nitrogen removal via nitrification and denitrification: extensions to general ASM models. Environ. Sci. Technol. 45 (2011) 7768-7776.

[36] L.H. Smith, P.L. McCarty, P.K. Kitanidis, Spreadsheet method for evaluation of biochemical reaction rate coefficients and their uncertainties by weighted nonlinear least-squares analysis of the integrated Monod equation. Appl. Environ. Microbial. 64 (1998) 2044-2050.

[37] S. Dannenberg, M. Kroder, W. Dilling, H. Cypionka, Oxidation of H_2, organic compounds and inorganic sulfur compounds coupled to reduction of O_2 or nitrate by sulfate-reducing bacteria. Arch. Microbial. 158 (1992) 93-99.

[38] X.J. Xu, C. Chen, A.J. Wang, H.L. Guo, Y. Yuan, D.J. Lee, N.Q. Ren, Kinetics of nitrate and sulfate removal using a mixed microbial culture with or without limited-oxygen fed. Appl. Microbial. Biotechnol. 98 (2014) 6115-6124.

[39] A.H. Stouthamer, Dissimilatory reduction of oxidized nitrogen compounds. In Biology of Anaerobic Microorganisms, ed. A.J.B. Zehnder. John Wiley & Sons, New York, NY (1988).

[40] C. Chen, N.Q. Ren, A.J. Wang, L.H. Liu, D.J. Lee, Enhanced performance of denitrifying sulfide removal process under micro-aerobic condition. J. Hazard. Mater. 179 (2010) 1147–1151.

[41] G. Muyzer, A.J.M. Stams, The ecology and biotechnology of sulfate-reducing bacteria. Nat. Rev. Microbial. 6 (2008) 441-454.

[42] A.E. Tugtas, U. Tezel, S.G. Pavlostathis, A comprehensive model of simultaneous denitrification and methanogenic fermentation processes. Biotechnol. Bioeng. 105 (2010) 98-108.

[43] C. Huilinir, E. Aspe, J.P. Delgenes, R. Moletta, Model of simultaneous denitrification and methanogenesis in an upflow packed-bed biofilm reactor: nitrogen compounds' inhibition and pseudo two-dimensional biofilm model. Journal of Chemical Technology and Biotechnology, 84 (2008) 254-268.

[44] T. Dalsgaard, F. Bak, Nitrate reduction in a sulfate-reducing bacterium, Desulfovibrio desulfuricans, isolated from rice paddy soil: sulfide inhibition, kinetics, and regulation. Appl. Environ. Microbial. 60 (1994) 291-297.

[45] D.J. Batstone, P.F. Pind, I. Angelidaki, Kinetics of thermophilic, anaerobic oxidation of straight and branched chain butyrate and valerate. Biotechnol. Bioeng. 84 (2003) 195-204.

[46] R. Von Schulthess, W. Gujer, Release of nitrous oxide (N_2O) from denitrifying activated sludge: Verification and application of a mathematical model. Water Res. 30 (1996) 521–530.

[47] J. Cai, P. Zheng, M. Qaisar, Influence of various nitrogenous electron acceptors on the anaerobic sulfide oxidation. Bioresour. Technol. 101 (2010) 2913–2937.

[48] X.J. Xu, C. Chen, A.J. Wang, W.Q. Guo, X. Zhou, D.J. Lee, N.Q. Ren, J.S. Chang, Simultaneous removal of sulfide, nitrate and acetate under denitrifying sulfide removal condition: modeling and experimental validation. J. Hazard. Mater. 264 (2014) 16-24.

[49] APHA, Standard Methods for the Examination of Water and Wastewater, 19th ed.

American Public Health Association, New York (1995).

[50] W.F. Lin, Z.S. Yu, H.X. Zhang, I.P. Thompson, Diversity and dynamics of microbial communities at each step of treatment plant for potable water generation. Water Res. 52 (2014) 218-230.

[51] G.H. Xu, F.J. Yin, S.H. Chen, Y.J. Xu, H.Q. Yu, Mathematical modeling of autotrophic denitrification (AD) process with sulfide as electron donor. Water Res. 91 (2016) 225-234.

[52] L. Rieger, S. Gillot, G. Langergraber, A. Shaw, Good Modelling Practice: Guidelines for Use of Activated Sludge Models. IWA Publishing, 2012.

[53] A.J. Wang, C.S. Liu, H.J. Han, D.J. Lee, Simultaneous removal of sulfide, nitrate and acetate: kinetic modeling. J. Hazard. Mater. 178 (2010) 35-41.

[54] Y. Tang, A.O. Valencia, L. Feng, C. Zhou, R. Krajmalnik-Brown, B.E. Rittmann, A biofilms model to understand the onset of sulfate reduction in denitrifying membrane biofilm reactors. Biotechnol. Bioeng. 110 (2013) 763-772.

[55] V. Fedorovich, P. Lens, S. Kalyuzhnyi, Extension of anaerobic digestion model No. 1 with processes of sulfate reduction. Appl. Biochem. Biotechnol. 109 (2003) 33-45.

Figure Captions

Fig. 1. Simplified representation of the biochemical process associated with carbon, nitrogen and sulfur conversions. The red line and green line represents the process described in ADM and ASM model respectively, and the black line represents the process extended in our model. The dotted line represents the process induced by oxygen fed.

Fig. 2. Model evaluation applied to Culture 1 (real data, symbols; model predications, lines): sulfate, nitrate, sulfide, lactate, acetate and methane profiles at initial nitrate concentration (mg L^{-1}) of 500 (A-B) as model calibration, 200 (C-D) and 700 (E-F) as model validation.

Fig. 3. Model evaluation applied to Culture 2 (real data, symbols; model predications, lines): sulfate, nitrate, sulfide, sulfur, lactate, acetate, methane and oxygen (30 ^{o}C, 1 atm) profiles at initial R_{OS} of 1.16 (A-B) as model calibration, 0.39 (C-D) and 1.93 (E-F) as model validation.

Fig. 4. The 95% confidence ellipsoids for kinetic parameters combinations in this model. Culture 1: A, B; Culture 2: C, D.

Fig. 5. Model application for (A) Sulfate-Reduction, Sulfide-Oxidation (SR-SO), and (B) Denitrifying Sulfide Removal (DSR) processes. For SR-SO process, the initial substrate concentrations are SO_4^{2-} = 616.8 mg L^{-1}, and added oxygen volume = 46 mL (molar ratio of oxygen to sulfide, R_{OS} = 2.0). For DSR process, the initial substrates concentrations are S^{2-} = 538.5 mg L^{-1}, NO_3^--N = 313.1 mg L^{-1}, and Ac^- = 899.7 mg L^{-1}. Both experiments were conducted in 300-mL sealed reactors and detailed operating information was the same as that in Culture 1 and 2.

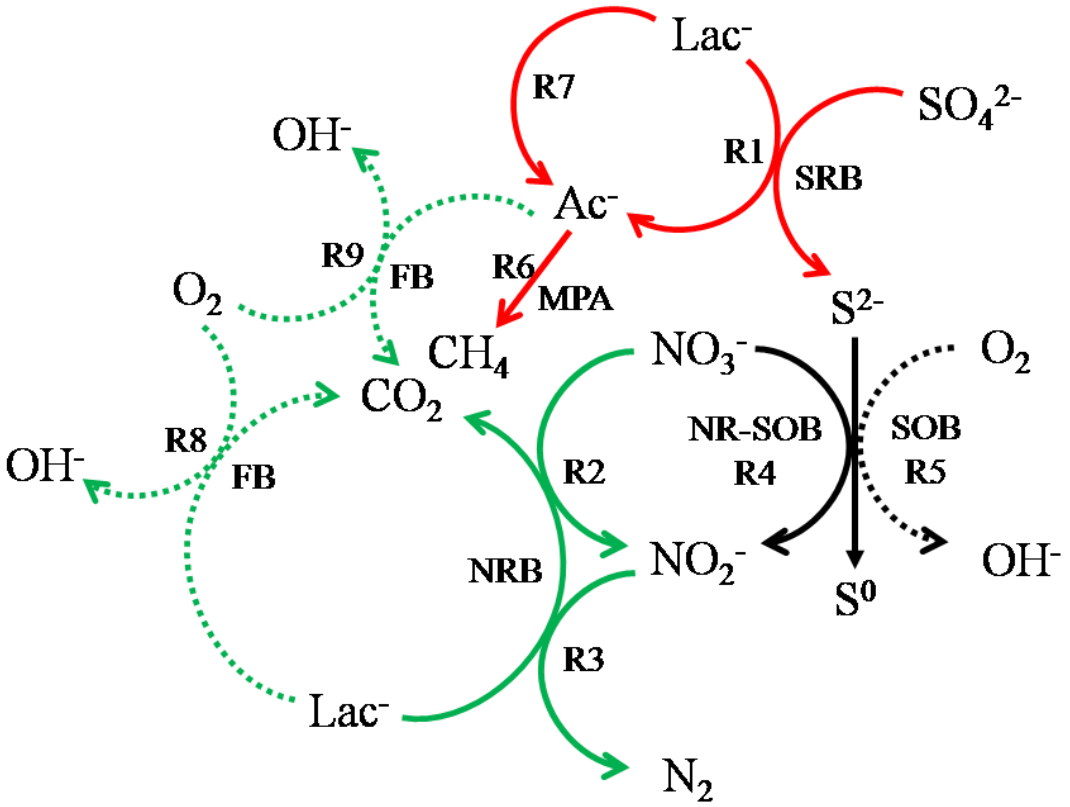

Fig. 1. Simplified representation of the biochemical process associated with carbon, nitrogen and sulfur conversions. **The red line** and **green line** represents the process described in ADM and ASM model respectively, and **the black line** represents the process extended in our model. The dotted line represents the processes induced by oxygen.

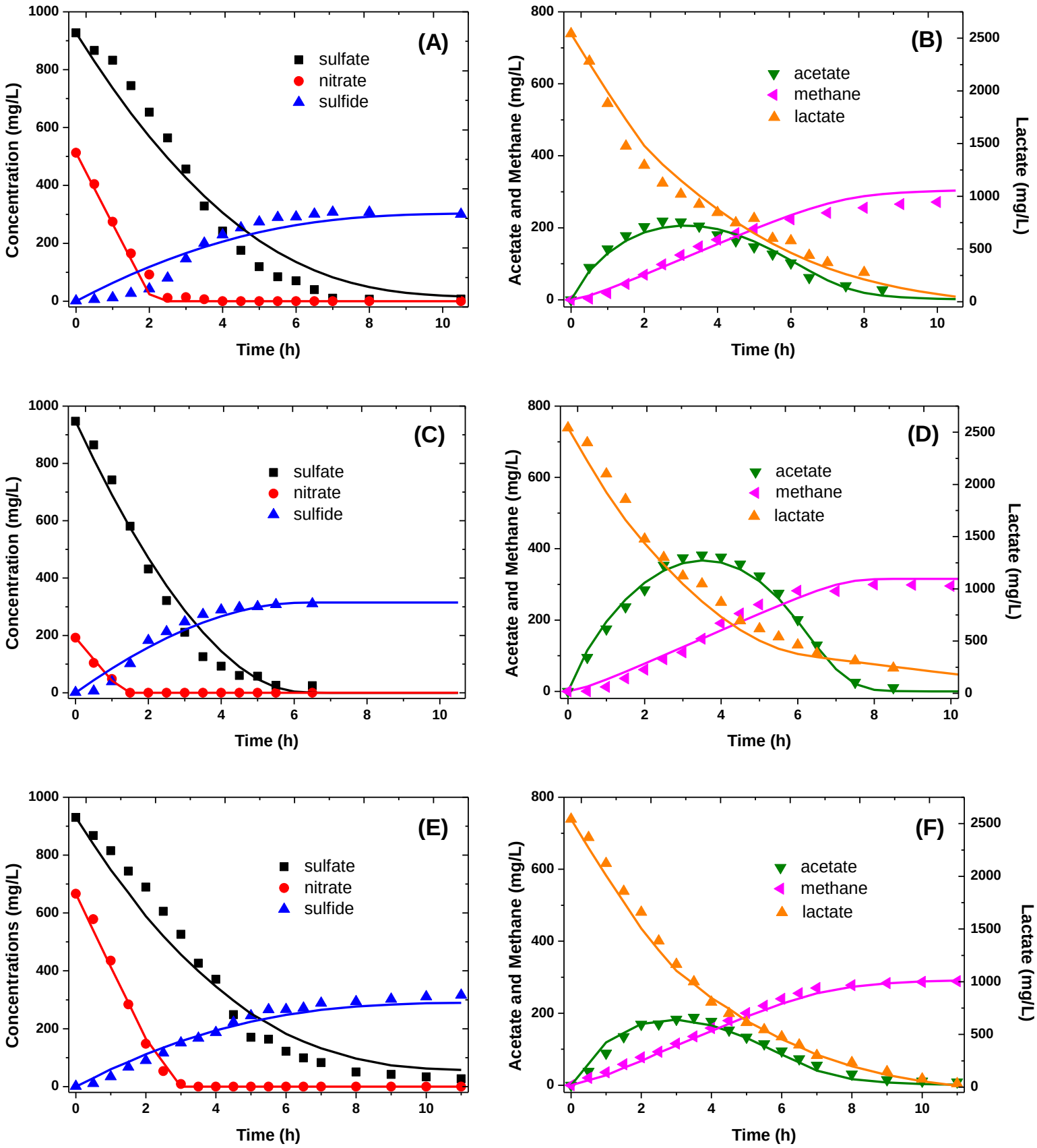

Fig. 2. Model evaluation applied to Culture 1 (real data, symbols; model predications, lines): sulfate, nitrate, sulfide, lactate, acetate and methane profiles at initial nitrate concentration (mg L^{-1}) of 500 (A-B) as model calibration, 200 (C-D) and 700 (E-F) as model validation.

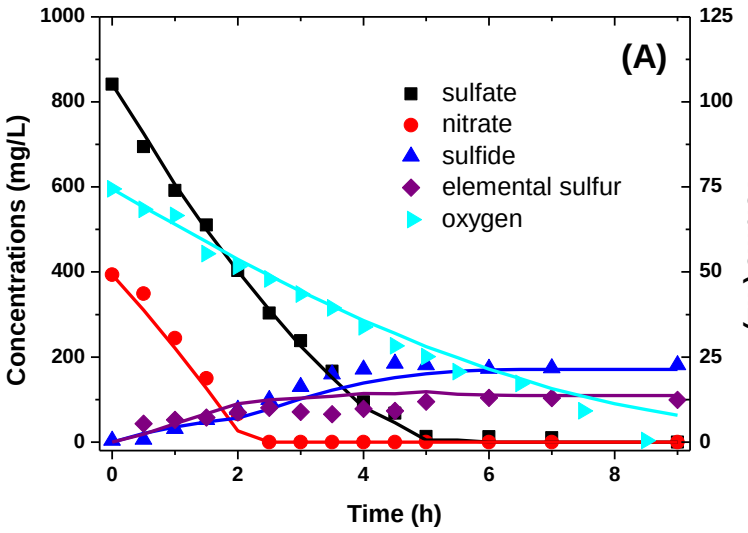

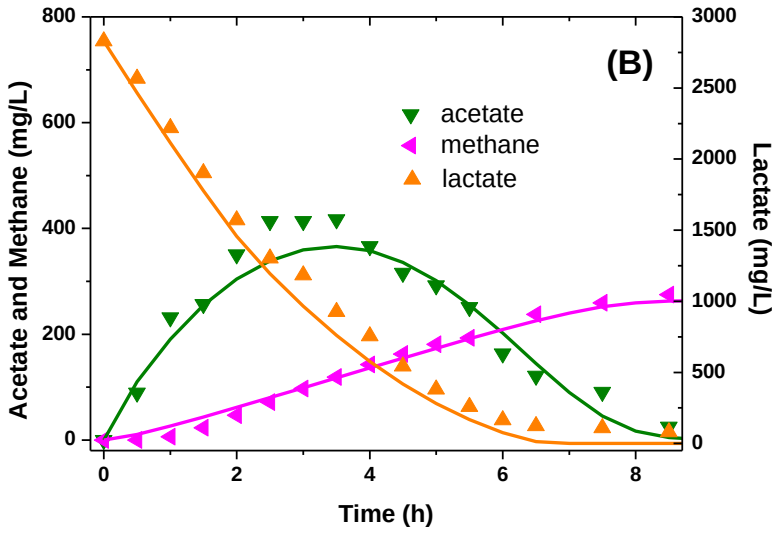

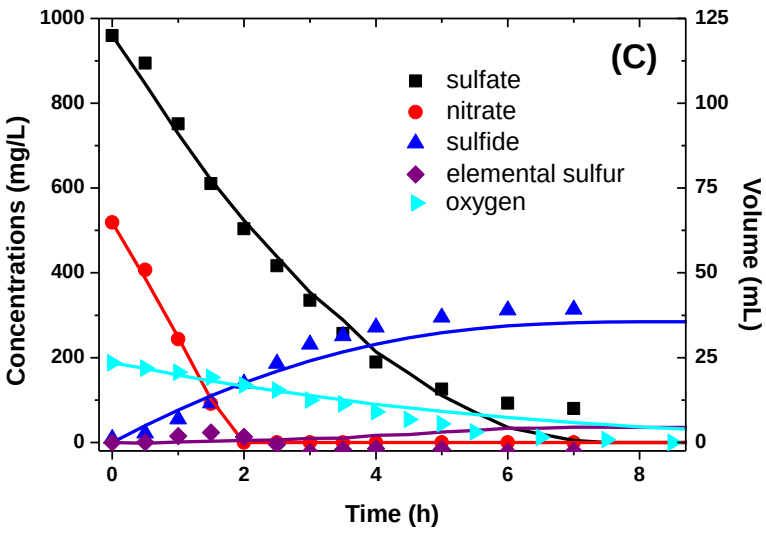

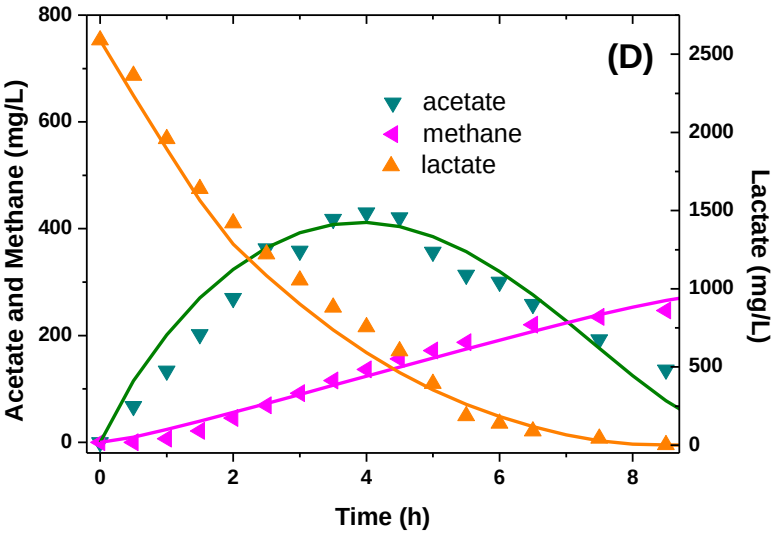

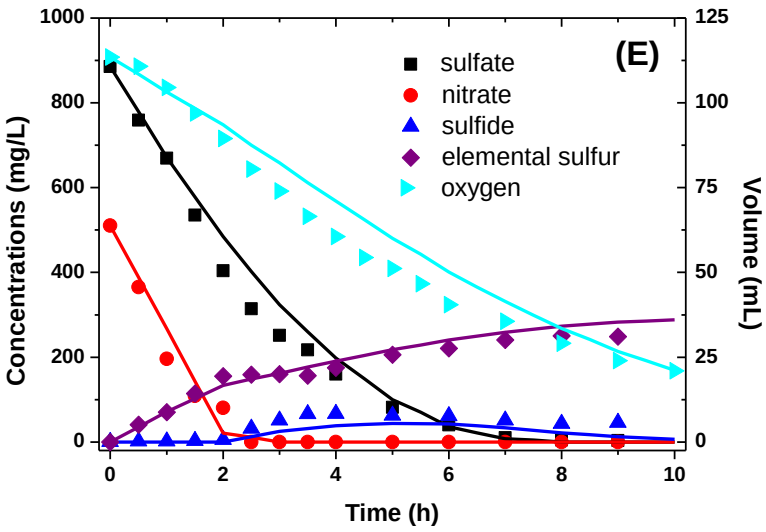

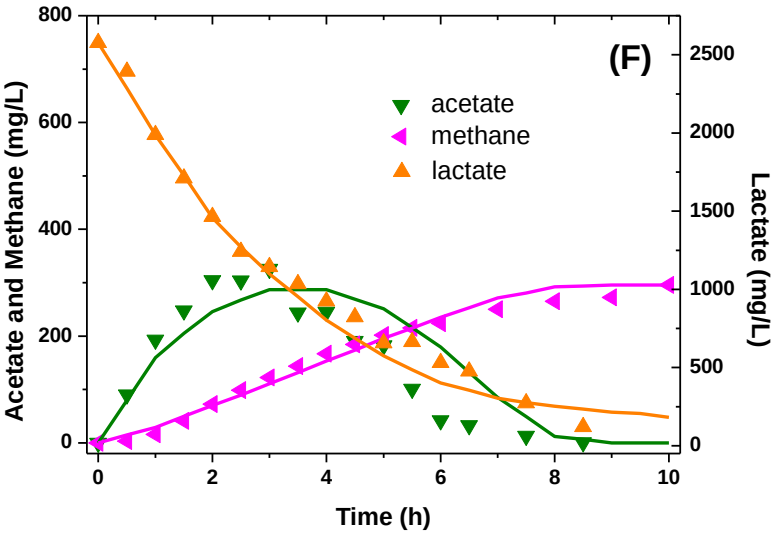

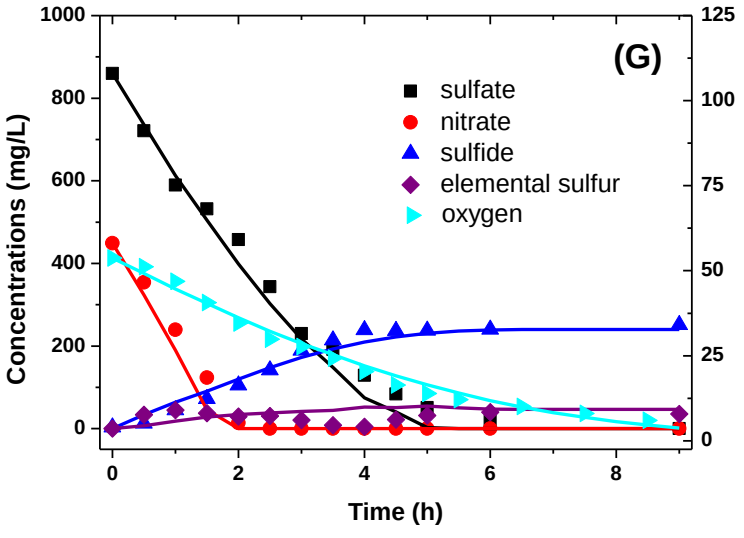

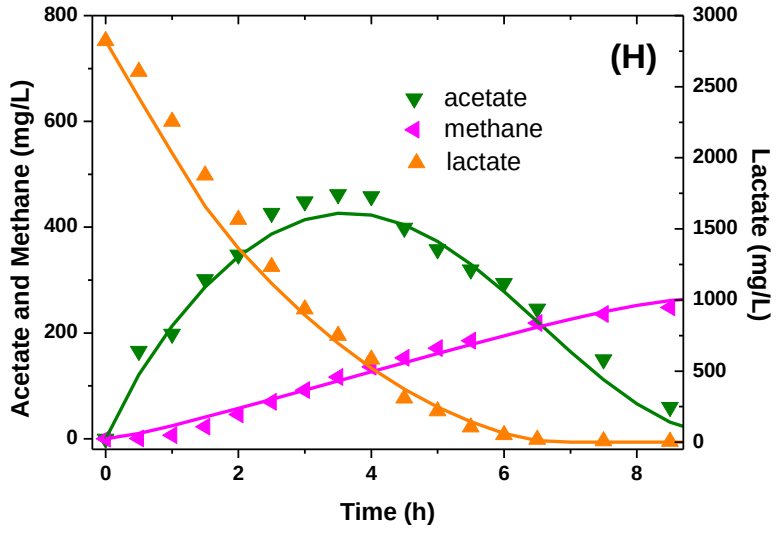

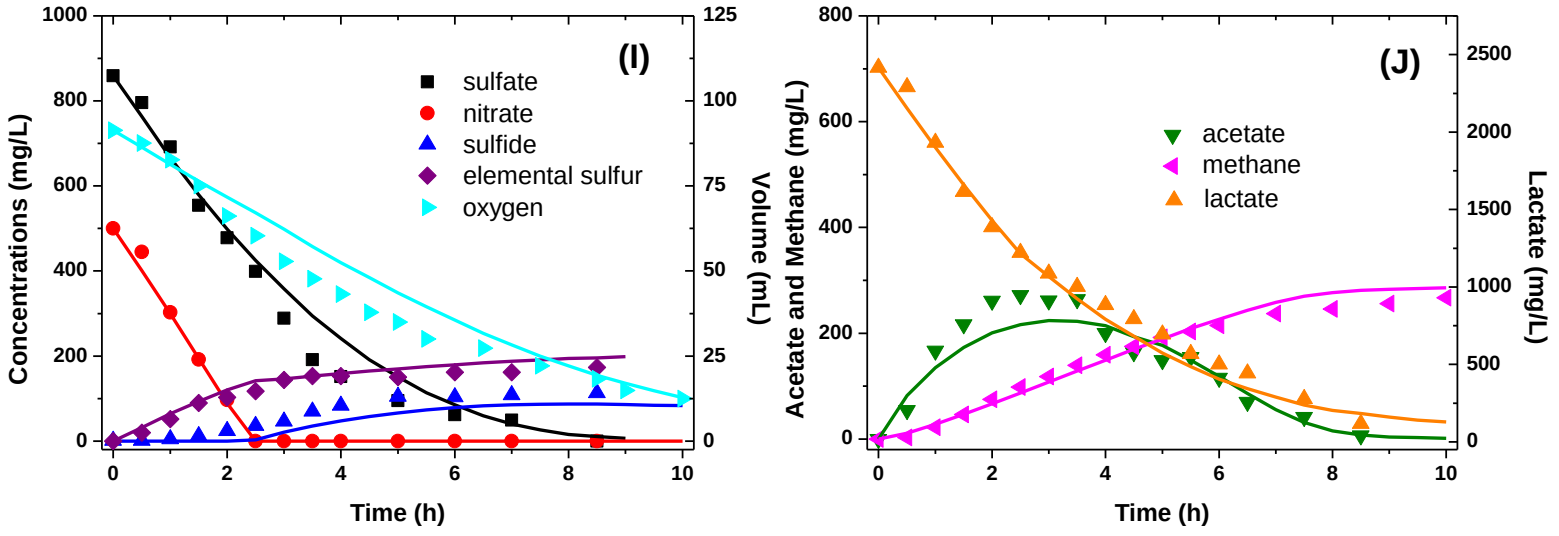

Fig. 3. Model evaluation applied to Culture 2 (real data, symbols; model predications, lines): sulfate, nitrate, sulfide, sulfur, lactate, acetate, methane and oxygen (30 ^{o}C, 1 atm) profiles at initial R_{OS} of 1.16 (A-B) as model calibration, 0.39 (C-D), 1.93 (E-F), 0.77 (G-H) and 1.55 (I-J) as model validation.

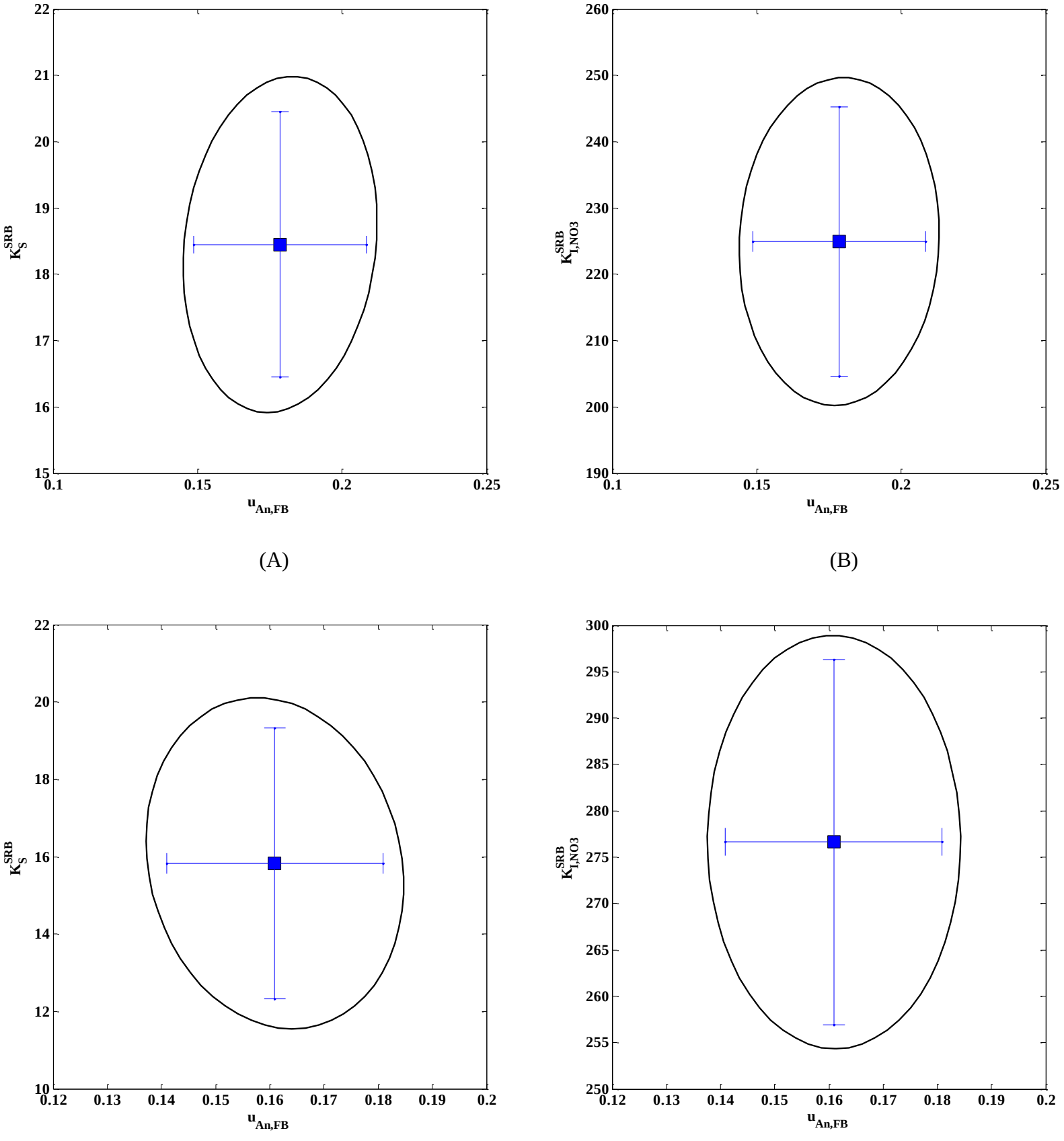

Fig. 4. The 95% confidence ellipsoids for kinetic parameters combinations in this model. Culture 1: A, B; Culture 2: C, D.

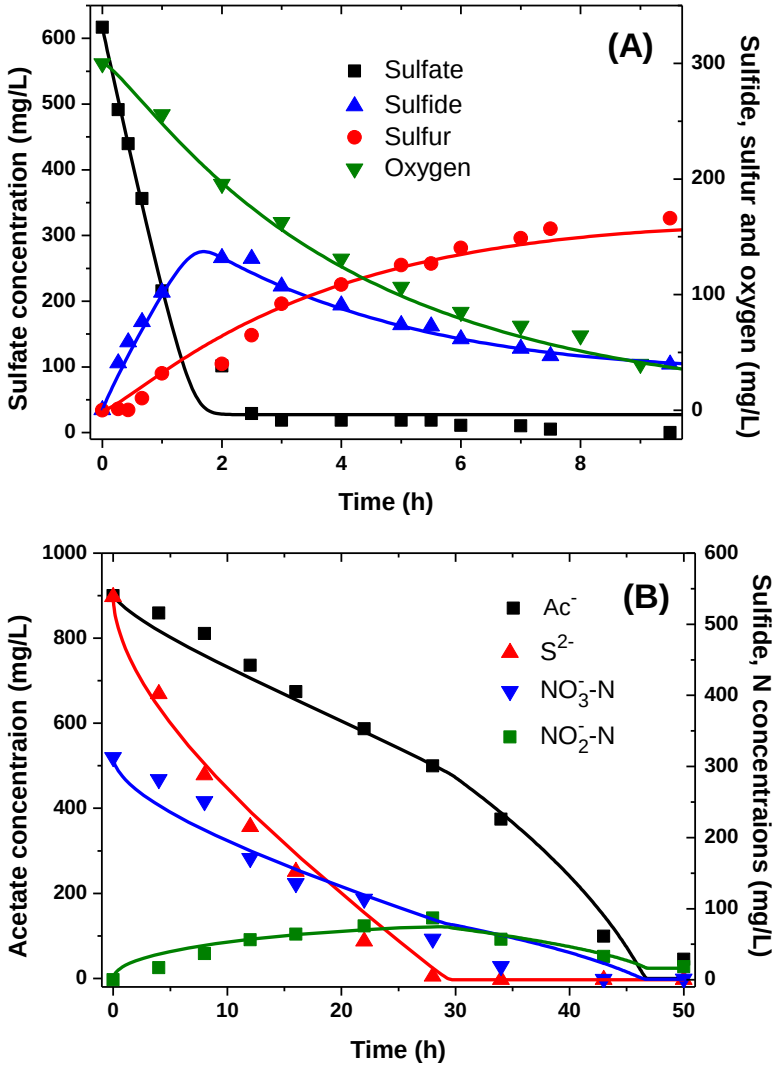

Fig. 5. Model application for (A) Sulfate Reduction-Sulfide Oxidation (SR-SO), and (B) Denitrifying Sulfide Removal (DSR) processes. For SR-SO process, the initial substrate concentrations are SO_4^{2-} = 616.8 mg L^{-1}, and added oxygen volume = 46 mL (molar ratio of oxygen to sulfide, R_{OS} = 2.0). For DSR process, the initial substrates concentrations are S^{2-} = 538.5 mg L^{-1}, NO_3^--N = 313.1 mg L^{-1}, and Ac^- = 899.7 mg L^{-1}. Both experiments were conducted in 300-mL sealed reactors and detailed operating information was the same as that in Culture 1 and 2.

Table 1. Experimental Conditions Applied in Batch Tests Culture 1 and 2

test	Organic carbon[a]	Nitrate	Sulfate		Oxygen		R_{OS}
	(mg L^{-1})	(mg L^{-1})	(mg L^{-1})	(mmol)	(mL)	(mmol)	
Culture 1	2700	200	1000	-	-	-	-
	2700	500	1000	-	-	-	-
	2700	700	1000	-	-	-	-
Culture 2	2700	500	1000	2.08	20	0.82	0.39
	2700	500	1000	2.08	40	1.64	0.77
	2700	500	1000	2.08	60	2.46	1.16
	2700	500	1000	2.08	80	3.28	1.55
	2700	500	1000	2.08	100	4.10	1.93

[a]Organic carbon concentrations were measured as chemical oxygen demand (COD). In this study lactate was used as organic carbon and was always kept above the limiting condition.

Table 2. Process matrix related to simultaneous C-N-S removal

process (j)		coefficient of component i in process j (η_{ij})															conversion rate (R_j)
		solid component						dissolved component									
		SRB	NRB	SOB	MPA	FB	IB	SO_4^{2-}	NO_3^-	NO_2^-	S^{2-}	S^0	Lactate	Acetate	CH_4	O_2	
SRB	growth	1						$\frac{Y_{SRB}-1}{1.875Y_{SR}}$			$\frac{1-Y_{SRB}}{5.625Y_{SR}}$		$-\frac{1}{Y_{SRB}}$	$\frac{1-Y_{SRB}}{1.5Y_{SRB}}$			$\mu_{SRB}f_{SRB}X\frac{S_{SO4}}{K_{SO4}^{SRB}\left(1+\frac{S_{NO3}}{K_{I,NO3}^{SRB}}\right)+S_{SO4}}\frac{S_S}{K_S^{SRB}}$
	endogenous decay	-1					$1-f_d$										$b_{SRB}f_{SRB}X$
NRB	growth on NO_3^-		1						$\frac{Y_{NRB}-1}{0.242Y_{NR}}$	$\frac{1-Y_{NRB}}{0.326Y_{NR}}$			$-\frac{1}{Y_{NRB}}$				$\mu_{NRB}^{NO3}f_{NRB}X\frac{S_{NO3}}{K_{NO3}^{NRB}(1+\frac{S_1}{K_{I,SO4}^{NRB}})+S_{NO3}}\frac{S_S}{K_S^{NRB1}}$
	growth on NO_2^-									$\frac{Y_{NRB}-1}{0.489Y_{NR}}$			$-\frac{1}{Y_{NRB}}$				$\mu_{NRB}^{NO2}f_{NRB}X\frac{S_{NO2}}{K_{NO2}^{NRB}+S_{NO2}}\frac{S_S}{K_S^{NRB2}+S_S}\frac{K_{I,O}^{N}}{K_{I,O2}^{NRB}}$
	endogenous decay		-1				$1-f_d$										$b_{NRB}f_{NRB}X$
SOB	growth on NO_3^-			1					$\frac{Y_{SOB}-1}{1.29Y_3}$		$-\frac{1}{Y_{SOB}}$	$\frac{1-Y_{SOB}}{Y_{SOB}}$					$\mu_{SOB}^{NO3}f_{SOB}X\frac{S_{NO3}}{K_{NO3}^{SOB}+S_{NO3}}\frac{S_{S2}}{K_{S2}^{SOB1}+S_{S2}}$
	growth on O_2			1							$-\frac{1}{Y_{SOB}}$	$\frac{1-Y_{SOB}}{Y_{SOB}}$				$\frac{Y_{SOB}-}{2Y_{SOB}}$	$\mu_{SOB}^{O2}f_{SOB}X\frac{S_{O2}}{K_{O2}^{SOB}+S_{O2}}\frac{S_{S2}}{K_{S2}^{SOB2}+S_{S2}}$
	endogenous decay			-1			$1-f_d$										$b_{SOB}f_{SOB}X$
MPA	growth				1									$-\frac{1}{Y_{MPA}}$	$\frac{1-Y_{MP}}{3.75Y_{MP}}$		$\mu_{MPA}f_{MPA}X\frac{S_{AC}}{K_{AC}^{MPA}+S_{AC}}\frac{K_{I,O2}^{MPA}}{K_{I,O2}^{MPA}+S_{O2}}\frac{K_{I,}^{M}}{K_{I,H2S}^{MPA}}$
	endogenous decay				-1		$1-f_d$										$b_{MPA}f_{MPA}X$
FB	anaerobic growth					1							$-\frac{1}{Y_{FB}}$	$\frac{1-Y_{FB}}{Y_{FB}}$			$\mu_{An,FB}f_{FB}X\frac{S_S}{K_S^{FB}+S_S}$
	microaerophilic growth					1							$-\frac{1}{Y_{FB}}$			$\frac{Y_{FB}-1}{0.938Y_F}$	$\mu_{Ox,FB}f_{FB}X\frac{S_{O2}}{K_{O2}^{FB}+S_{O2}}\frac{S_S}{K_S^{FB}+S_S}$
						1								$-\frac{1}{Y_{FB}}$		$\frac{Y_{FB}-1}{0.938Y_F}$	$\mu_{Ox,FB}f_{FB}X\frac{S_{O2}}{K_{O2}^{FB}+S_{O2}}\frac{S_{AC}}{K_{AC}^{FB}+S_{AC}}$

endogenous decay	-1	$1 - f_d$	$b_{FB}f_{FB}X$

Table 3. Kinetic and stoichiometric parameters of the model

Parameter	Definition	Values	Unit	Source
Kinetic parameters				
μ_{SRB}	maximum specific growth rate of SRB	0.061	h^{-1}	(3)
μ_{NRB}^{NO3}	maximum S_{NO3}-mediated specific growth rate of NRB	0.053	h^{-1}	(2)
μ_{NRB}^{NO2}	maximum S_{NO2}-mediated specific growth rate of NRB	0.056	h^{-1}	(2)
μ_{SOB}^{NO3}	maximum S_{NO3}-mediated specific growth rate of SOB	0.245	h^{-1}	(8)
μ_{SOB}^{O2}	maximum S_{O2}-mediated specific growth rate of SOB	0.028	h^{-1}	(7)
μ_{MPA}	maximum specific growth rate of MPA	0.005	h^{-1}	(6)
$\mu_{An,FB}$	maximum specific anaerobic growth rate of FB	0.18 ± 0.03	h^{-1}	(1)
$\mu_{Ox,FB}$	maximum specific aerobic growth rate of FB	0.25	h^{-1}	(5)
K_{SO4}^{SRB}	S_{SO4} affinity constant for SRB	6.67	mg S L^{-1}	(3)
K_{NO3}^{NRB}	S_{NO3} affinity constant for NRB	0.251	mg N L^{-1}	(2)
K_{NO2}^{NRB}	S_{NO2} affinity constant for NRB	0.810	mg N L^{-1}	(2)
K_{NO3}^{SOB}	S_{NO3} affinity constant for SOB	0.20	mg N L^{-1}	(4)
K_{S2}^{SOB1}	S_{S2} affinity constant for S_{NO3}-mediated SOB	1.36	mg S L^{-1}	(4)
K_{S2}^{SOB2}	S_{S2} affinity constant for S_{O2}-mediated SOB	11.0	mg S L^{-1}	(7)
K_{S}^{SRB}	S_S affinity constant for SRB	18.5 ± 2.0	mg COD L^{-1}	(1)
K_{S}^{NRB1}	S_S affinity constant for S_{NO3}-mediated NRB	5.0	mg COD L^{-1}	(2)
K_{S}^{FB}	S_S affinity constant for FB	20.0	mg COD L^{-1}	(5)
K_{S}^{NRB2}	S_S affinity constant for S_{NO2}-mediated NRB	1.5	mg COD L^{-1}	(2)
K_{AC}^{MPA}	S_{AC} affinity constant for MPA	52.5	mg COD L^{-1}	(6)
K_{O2}^{SOB}	S_{O2} affinity constant for SOB	200	mg $O_2 L^{-1}$	(7)
K_{O2}^{FB}	S_{O2} affinity constant for FB	0.2	mg $O_2 L^{-1}$	(5)
$K_{I,NO3}^{SRB}$	S_{NO3} inhibiting coefficient for SRB	225.8 ± 20.3	mg N L^{-1}	(1)
$K_{I,SO4}^{NRB}$	S_{SO4} inhibiting coefficient for NRB	327.3 ± 68.7	mg S L^{-1}	(1)

$K_{I,O2}^{NRB}$	S_{O2} inhibiting coefficient for NRB	0.588	mg O_2L^{-1}	(1)
$K_{I,O2}^{SRB}$	S_{O2} inhibiting coefficient for SRB	-	mg O_2L^{-1}	(1)
$K_{I,O2}^{MPA}$	S_{O2} inhibiting coefficient for MPA	-	mg O_2L^{-1}	(1)
$K_{I,H2S}^{MPA}$	S_{H2S} inhibiting coefficient for MPA	0.285	g S L^{-1}	(6)
b_{SRB}	inactivation coefficient for SRB	0.035	h^{-1}	(3)
b_{NRB}	inactivation coefficient for NRB	0.026	h^{-1}	(5)
b_{SOB}	inactivation coefficient for SOB	10^{-5}-10^{-6}	h^{-1}	(8)
b_{MPA}	inactivation coefficient for MPA	0.0155	d^{-1}	(6)
b_{FB}	inactivation coefficient for FB	0.62	d^{-1}	(5)
Stoichiometric parameters				
Y_{SRB}	yield coefficient for SRB	0.54	g VSS g^{-1} COD	(3)
Y_{NRB}	yield coefficient for NRB	0.67	g VSS g^{-1} COD	(5)
Y_{SOB}	yield coefficient for SOB	0.090	g VSS g^{-1} S^{2-}	(7)
Y_{MPA}	yield coefficient for MPA	0.026	g VSS g^{-1} COD	(6)
Y_{FB}	Yield coefficient for FB	0.67	g VSS g^{-1} COD	(5)
f_d	fraction of biomass that is biodegradable	0.8	-	(5)

Source: (1) this study (Culture 1); (2) von Schulthess and Gujer [46]; (3) Moosa et al. [21]; (4) Cai et al. [47]; (5) Henze et al. [18]; (6)Kalyuzhnyi and Fedorovich [19]; (7) Xu et al. [28]; (8) Xu et al. [48]